Plane Wave Diffraction by Arbitrary-Angled Lossless Wedges: High Frequency and Time Domain Solutions

M. Frongillo, G. Gennarelli, and G. Riccio, *Member*, *IEEE*

***Abstract*—This paper concerns the diffraction phenomenon originated by a uniform plane wave impacting an arbitrary-angled lossless dielectric wedge with planar surfaces. The high frequency diffraction coefficients are obtained by performing uniform asymptotic evaluations of the radiation integrals resulting from the physical optics approximation of the electric and magnetic equivalent surface currents located on the inner and outer faces of the wedge. The final expressions are in closed form and contain the standard transition function of the uniform theory of diffraction and the Fresnel reflection and transmission coefficients related to the geometrical optics propagation mechanisms. Moreover they allow a simple physical interpretation of each contribution and they are easy to use and to implement in a computer code. The knowledge of such diffraction coefficients in the frequency domain permits to apply the inverse Laplace transform to obtain the time domain counterparts, which enable the evaluation of the transient diffracted field originated by an arbitrary function plane wave.**

***Index Terms*—Propagation, Diffraction, Wedge, Frequency Domain, Time Domain.**

I. Introduction

Asymptotic methods based on ray tracing are more attractive and efficient than numerical techniques when solving high frequency scattering problems. This statement is well-known to researchers and electromagnetic engineers working on radio planning, analysis and design of antennas, through-wall building imaging, and so forth. Their activities usually benefit from the use of the Geometrical Theory of Diffraction (GTD) [1] and its uniform version (UTD) [2], which describe the electromagnetic (EM) wave propagation in terms of incident, reflected, transmitted and diffracted rays. Such ray-based methods allow one to solve a large number of real scattering problems by using the solutions of a reduced number of simple canonical problems. Moreover, they provide physical insight into the radiation and scattering mechanisms arising from the various parts of the structure. Unfortunately the applicability of ray-based methods to penetrable structures suffers from the absence of a closed form exact solution to the canonical diffraction problem involving a dielectric wedge. This is a challenging problem and the boundary conditions matching at the wedge interfaces represents an obstacle to solve it. Several analytical and heuristic approximate solutions have been proposed in the past few decades, as well as procedures combining analytical and numerical techniques for solving the diffraction problem in an exact sense. Although of great interest from theoretical viewpoint, some of them have limited applicability owing their low computation efficiency. Representative studies on diffraction by dielectric wedges are reported in [3]-[18].

Frequency domain Uniform Asymptotic Physical Optics (FD-UAPO) solutions have been recently proposed in the UTD framework to evaluate the diffraction coefficients relevant to plane waves impacting right- and obtuse-angled lossless dielectric (i.e., electric and magnetic parameters are considered real) wedges [16], [17]. The corresponding time domain (TD-UAPO) counterparts have been obtained in [19] and [20] by using the inverse Laplace transform according to [21]. The approach has been successively applied to acute-angled wedges in the case of incidence directions able to generate internal rays running away from the edge [18], [22]. It must be stressed that no attention has been devoted in [18], [22] to the internal rays bouncing toward the edge when the grazing angle is less than 90°. Note that FD-UAPO solutions can be obtained also in the case of lossy dielectrics [23].

The FD-UAPO solutions are in closed form and include the Geometrical Optics (GO) response of the structure and the UTD transition function [2]. Moreover, although they suffer from well-known limitations due to the PO approximation, they provide quite accurate results when compared with numerical tools.

This manuscript contains the FD- and TD-UAPO generalized solutions for the canonical diffraction problems associated to uniform plane waves impacting lossless dielectric wedges with arbitrary apex angle and dielectric constant. The reported analysis is complete. It permits to solve the diffraction problems in [16]-[18], [19], [20], and [22] as particular cases. The approach splits the observation region into the space filled by the dielectric (internal region) and the surrounding free-space (external region). Multiple internal

M. Frongillo is with Railway-Research srl, via Vicinale S. Maria del Pianto – Torre 1, 80143 Napoli, Italy (e-mail: marcello.frongillo@railway-research.it).

G. Gennarelli is with the Institute for Electromagnetic Sensing of the Environment, National Research Council, via Diocleziano 328, 80124 Naples, Italy (e-mail: gennarelli.g@irea.cnr.it).

G. Riccio is with the Department of Information and Electrical Engineering and Applied Mathematics, University of Salerno, via Giovanni Paolo II 132, 84084 Fisciano (SA), Italy (e-mail: griccio@unisa.it).

reflections and external transmissions are considered to evaluate the GO field at any observation point when the incidence direction of the plane wave is fixed. In particular, the knowledge of the GO field along the internal (external) faces of the wedge allows one to determine the electric and magnetic equivalent PO surface currents to be used in the radiation integral related to the internal (external) problem. For each observation region, the surface radiation integral is given by the sum of the two contributions due to the involved wedge faces. Useful analytical approximations, manipulations and evaluations permit to obtain integrals able to be solved by means of the Steepest Descent Method and the Multiplicative Method. The result of the above procedure is a closed form approximate solution for the diffracted field in the UTD framework. It must be stressed that the obtained FD-UAPO solutions for the internal and external regions should be not considered as "reference", but as "approximate, reliable and user-friendly" solutions accessible to EM engineers. The TD-UAPO counterparts are then obtained by using the inverse Laplace transform under the hypothesis that the dielectric parameters are independent on the frequency. Preliminary analysis and tests have been carried out in [24], [25].

This paper is organized as follows. Section II includes the ray tracing analysis and the GO field evaluation into the internal and external regions when the incidence direction of the plane wave is fixed. The FD-UAPO expressions of the field diffracted by the edge are presented in Section III, where a representative set of numerical examples is reported to show their effectiveness. Section IV provides the TD-UAPO diffraction coefficients relevant to the transient diffracted field originated by a plane wave with a specific time variation. Conclusions and remarks are collected in Section V.

II. Geometrical Optics Field

The considered canonical problem deals with the plane wave propagation in presence of a penetrable wedge described by the internal apex angle α and bounded by the planar surfaces S_0 and S_α. The wedge material is lossless and non-magnetic ($\mu_r = 1$), and ε_r is its real relative permittivity. The case $\alpha < \pi/2$ (see Fig. 1) is the most interesting since the GO propagation analysis involves multiple reflection/transmission mechanisms and contains the contributions arising when $\pi/2 \le \alpha < \pi$. Accordingly, $\alpha < \pi/2$ is considered from this point on.

The incidence direction is orthogonal to the edge and the incident electric field is $\underline{E}^i = E_0^i \exp(-j\underline{k}_0 \cdot \underline{r})\,\hat{z}$ (*E*-polarization), where $\underline{r} = \rho\cos\phi\,\hat{x} + \rho\sin\phi\,\hat{y}$ is the position vector of the observation point *P* and $\underline{k}_0 = k_0(-\cos\phi'\hat{x} - \sin\phi'\hat{y})$ is the free-space propagation vector. Three ranges of ϕ' values are examined in the following.

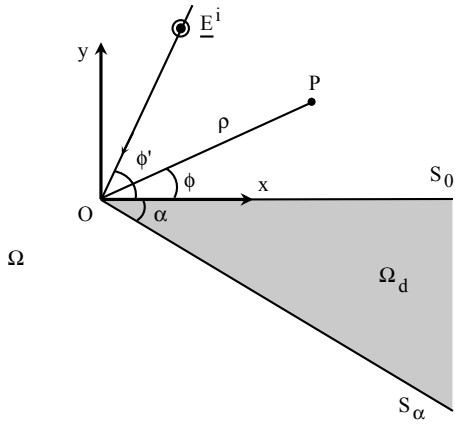

Fig. 1. Geometry of the problem.

A. $0 < \phi' < \pi/2$

The wave penetrates into the wedge according to the transmission angle $\theta_{0L}^t = \sin^{-1}(\sin\theta^i/\sqrt{\varepsilon_r})$, where $\theta^i = \pi/2 - \phi'$ at S_0, and originates multiple reflection and transmission contributions (see Fig. 2). The internal propagation is initially towards the edge (left propagation, *L*) and subsequently towards the unbounded side of the wedge (right propagation, *R*). This last part of the path starts at the interaction point on S_0 corresponding to the internal incidence angle $\theta_{N+1}^i = (N+1)\alpha - \theta_{0L}^t = \theta_{0R}^t$, where $N = N_i = \mathrm{Int}[\theta_{0L}^t/\alpha]$ if N_i is odd or $N = N_i + 1$ otherwise. If *P* is in the internal region (Ω_d), the GO field is:

$$
\begin{aligned}
\underline{E}^{GO}_{\Omega_d}(P) = \hat{z}\,E_0^i T_{0L}\Bigg\{\Bigg\{&\exp\left(jk_d\rho\sin\left(\phi+\theta_{0L}^t\right)\right)+\\
&+\sum_{\substack{n=1\\ n\ even}}^{N}\left(\prod_{p=1}^{n}R_{pL}\right)\exp\left(jk_d\rho\sin\left(\phi+\theta_{nL}^i\right)\right)+\\
&+\sum_{\substack{n=1\\ n\ odd}}^{N}\left(\prod_{p=1}^{n}R_{pL}\right)\exp\left(-jk_d\rho\sin\left(\phi-\theta_{nL}^i+\alpha\right)\right)\Bigg\}+\\
&+\Gamma(N)\Bigg\{\exp\left(jk_d\rho\sin\left(\phi-\theta_{0R}^t\right)\right)+\\
&+\sum_{\substack{m=1\\ m\ even}}^{M}\left(\prod_{p=1}^{m}R_{pR}\right)\exp\left(jk_d\rho\sin\left(\phi-\theta_{mR}^i\right)\right)+\\
&+\sum_{\substack{m=1\\ m\ odd}}^{M}\left(\prod_{p=1}^{m}R_{pR}\right)\exp\left(-jk_d\rho\sin\left(\phi+\theta_{mR}^i+\alpha\right)\right)\Bigg\}\Bigg\}
\end{aligned}
\tag{1}
$$

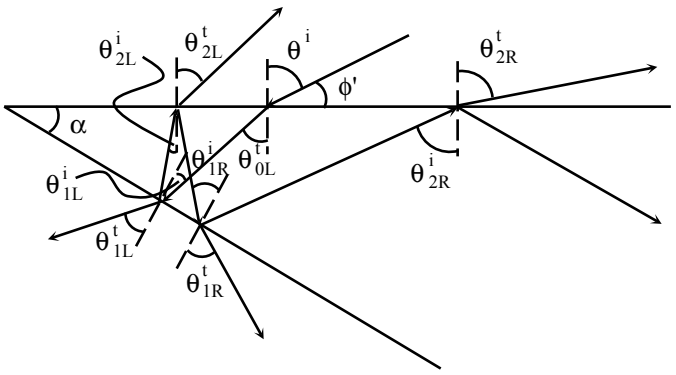

Fig. 2. Case *A*. GO field propagation.

where $\theta^i_{pL,R}$ is the internal incidence angle at the p-th interaction, M is the number of internal reflections related to the ray running towards the unbounded side of the wedge, R and T denote the reflection and transmission coefficients involved in the propagation mechanisms, $k_d = k_0\sqrt{\varepsilon_r}$, and

$$\Gamma(N) = \begin{cases} \prod_{p=1}^{N+1} R_p & \text{if } N_i \text{ is odd} \\ 0 & \text{if } N_i = 0 \\ U\left(\frac{\pi}{2} - \theta^t_{0R}\right)\prod_{p=1}^{N+1} R_p & \text{if } N_i \text{ is even} \end{cases} \tag{2}$$

with $U(\theta) = 1$ if $\theta > 0$ or $U(\theta) = 0$ otherwise.

Transmitted waves through S_0 and S_α exist until the total reflection occurs inside the wedge. Their shadow boundaries are fixed by the angles $\theta^t_{pL,R}$ in the space surrounding the wedge (see Fig. 2). Hence, if P is in the region Ω, which is external to the wedge, it results:

$$\begin{aligned} \underline{E}^{GO}_{\Omega}(P) = \hat{z}\, E^i_0 \Big\{ & \exp\left(jk_0\rho\cos(\phi-\phi')\right)W(0,\pi+\phi') + \\ & + R_{0L}\exp\left(jk_0\rho\cos(\phi+\phi')\right)W(0,\pi-\phi') + \\ & + T_{0L}\Big\{ \sum_{\substack{n=1 \\ n\ even}}^{N} T_{nL}\exp\left(-jk_0\rho\sin\left(\phi-\theta^t_{nL}\right)\right)\left(\prod_{p=1}^{n-1} R_{pL}\right)\times \\ & \times W\left(0,\frac{\pi}{2}+\theta^t_{nL}\right)U\left(\theta_c-\theta^i_{nL}\right) + \\ & + \sum_{\substack{n=1 \\ n\ odd}}^{N} T_{nL}\exp\left(jk_0\rho\sin\left(\phi+\alpha+\theta^t_{nL}\right)\right)\left(\prod_{p=1}^{n-1} R_{pL}\right)\times \\ & \times W\left(\frac{3\pi}{2}-\alpha-\theta^t_{nL},2\pi-\alpha\right)U\left(\theta_c-\theta^i_{nL}\right)\Big\} + \\ & + \Gamma(N)\Big\{ \sum_{\substack{m=1 \\ m\ even}}^{M} T_{mR}\exp\left(-jk_0\rho\sin\left(\phi+\theta^t_{mR}\right)\right)\left(\prod_{p=1}^{m-1} R_{pR}\right)\times \\ & \times W\left(0,\frac{\pi}{2}-\theta^t_{mR}\right)U\left(\theta_c-\theta^i_{mR}\right) + \\ & + \sum_{\substack{m=1 \\ m\ odd}}^{M} T_{mR}\exp\left(jk_0\rho\sin\left(\phi+\alpha-\theta^t_{mR}\right)\right)\left(\prod_{p=1}^{m-1} R_{pR}\right)\times \\ & \times W\left(\frac{3\pi}{2}-\alpha+\theta^t_{mR},2\pi-\alpha\right)U\left(\theta_c-\theta^i_{mR}\right)\Big\}\Big\} \end{aligned} \tag{3}$$

where, $\theta_c = \sin^{-1}(1/\sqrt{\varepsilon_r})$ is the internal critical angle and $W(\theta_1,\theta_2) = 1$ if $\theta_1 < \theta < \theta_2$ or $W(\theta_1,\theta_2) = 0$ otherwise.

B. $\pi/2 < \phi' < \pi - \alpha$

The transmission angle at S_0 is $\theta^t_{0R} = \sin^{-1}(\sin\theta^i/\sqrt{\varepsilon_r})$, with $\theta^i = \phi' - \pi/2$. The wave moves away from the apex generating multiple GO contributions inside and outside the wedge (see Fig. 3), thus obtaining

$$\begin{aligned} \underline{E}^{GO}_{\Omega_d}(P) = \hat{z}\, E^i_0 T_{0R}\Big\{ & \exp\left(jk_d\rho\sin\left(\phi-\theta^t_{0R}\right)\right) + \\ & + \sum_{\substack{m=1 \\ m\ even}}^{M}\left(\prod_{p=1}^{m} R_{pR}\right)\exp\left(jk_d\rho\sin\left(\phi-\theta^i_{mR}\right)\right) + \\ & + \sum_{\substack{m=1 \\ m\ odd}}^{M}\left(\prod_{p=1}^{m} R_{pR}\right)\exp\left(-jk_d\rho\sin\left(\phi+\theta^i_{mR}+\alpha\right)\right)\Big\} \end{aligned} \tag{4}$$

$$\begin{aligned} \underline{E}^{GO}_{\Omega}(P) = \hat{z}\, E^i_0 \Big\{ & \exp\left(jk_0\rho\cos(\phi-\phi')\right)W(0,\pi+\phi') + \\ & + R_{0R}\exp\left(jk_0\rho\cos(\phi+\phi')\right)W(0,\pi-\phi') + \\ & + T_{0R}\Big\{ \sum_{\substack{m=1 \\ m\ even}}^{M} T_{mR}\exp\left(-jk_0\rho\sin\left(\phi+\theta^t_{mR}\right)\right)\left(\prod_{p=1}^{m-1} R_{pR}\right) \\ & \times W\left(0,\frac{\pi}{2}-\theta^t_{mR}\right)U\left(\theta_c-\theta^i_{mR}\right) + \\ & + \sum_{\substack{m=1 \\ m\ odd}}^{M} T_{mR}\exp\left(jk_0\rho\sin\left(\phi+\alpha-\theta^t_{mR}\right)\right)\left(\prod_{p=1}^{m-1} R_{pR}\right)\times \\ & \times W\left(\frac{3\pi}{2}-\alpha+\theta^t_{mR},2\pi-\alpha\right)U\left(\theta_c-\theta^i_{mR}\right)\Big\}\Big\} \end{aligned} \tag{5}$$

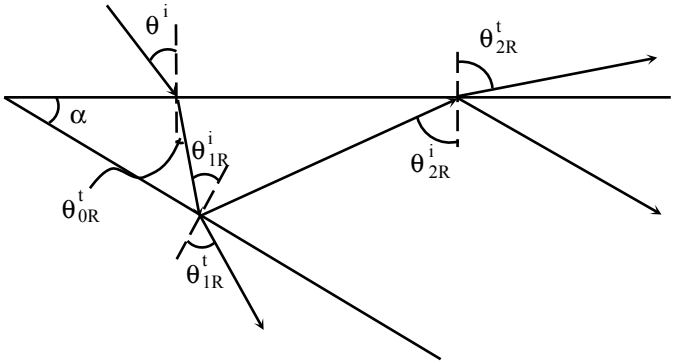

Fig. 3. Case *B*. GO field propagation.

C. $\pi-\alpha<\phi'<\pi$

The wave penetrates into the wedge through S_0 and S_α with transmission angles θ_{0R}^t and $\theta_{\alpha R}^t$, respectively. The GO field related to S_0 can be again evaluated by using Eqs. (4) and (5), whereas similar expressions can be derived to determine the contributions due to S_α.

III. FD-UAPO Diffracted Field

The goal is to find uniform expressions of the diffracted field able to compensate the GO field discontinuities and to provide an accurate total field evaluation in Ω_d and Ω. According to the equivalence principle, the scattered field $\underline{E}^s$ in Ω_d and Ω can be evaluated by means of the radiation integral containing the electric ($\underline{J}_s$) and magnetic ($\underline{J}_{ms}$) equivalent surface current densities, i.e.,

$$\underline{E}^s(P)\cong -jk\iint_S\left[\left(\underline{\underline{I}}-\hat{R}\hat{R}\right)\left(\zeta\,\underline{J}_s\right)+\underline{J}_{ms}\times\hat{R}\right]G(R)\,dS \tag{6}$$

with $G(R)=\exp(-jkR)/4\pi R=\exp(-jk|\underline{r}-\underline{r}'|)/4\pi|\underline{r}-\underline{r}'|$ if $\underline{r}'$ fixes the source point and $\hat{R}=(\underline{r}-\underline{r}')/|\underline{r}-\underline{r}'|$. The symbol $\underline{\underline{I}}$ denotes the 3x3 identity matrix and ζ is the intrinsic impedance of the material. Each term of the GO field formulation contributes to the $\underline{J}_s$ and $\underline{J}_{ms}$ expressions in the PO approximation, e.g., the GO field expressed by (4) gives:

$$\begin{aligned}\zeta_d\,\underline{J}_{s_0}=\hat{z}\,E_0^i T_{0R}\Bigg\{&-\exp\left(-jk_d\rho'\sin\theta_{0R}^t\right)\cos\theta_{0R}^t+\\&+\sum_{\substack{m=1\\ m\ even}}^{M}\left(\prod_{p=1}^{m-1}R_{pR}\right)\exp\left(-jk_d\rho'\sin\theta_{mR}^i\right)\times\\&\times\left(1-R_{mR}\right)\cos\theta_{mR}^i\Bigg\}\end{aligned} \tag{7}$$

$$\begin{aligned}\underline{J}_{ms_0}=\hat{x}\,E_0^i T_{0R}\Bigg\{&\exp\left(-jk_d\rho'\sin\theta_{0R}^t\right)+\\&+\sum_{\substack{m=1\\ m\ even}}^{M}\left(\prod_{p=1}^{m-1}R_{pR}\right)\exp\left(-jk_d\rho'\sin\theta_{mR}^i\right)\left(1+R_{mR}\right)\Bigg\}\end{aligned} \tag{8}$$

$$\begin{aligned}\zeta_d\,\underline{J}_{s_\alpha}=&-\hat{z}\,E_0^i T_{0R}\sum_{\substack{m=1\\ m\ odd}}^{M}\left(\prod_{p=1}^{m-1}R_{pR}\right)\exp\left(-jk_d\rho'\sin\theta_{mR}^i\right)\times\\&\times\Bigg\{\left[R_{mR}\sin\left(\theta_{mR}^i+\alpha\right)+\sin\left(\theta_{mR}^i-\alpha\right)\right]\sin\alpha+\\&+\left[R_{mR}\cos\left(\theta_{mR}^i+\alpha\right)-\cos\left(\theta_{mR}^i-\alpha\right)\right]\cos\alpha\Bigg\}\end{aligned} \tag{9}$$

$$\begin{aligned}\underline{J}_{ms_\alpha}=&\left[-\cos\alpha\,\hat{x}+\sin\alpha\,\hat{y}\right]E_0^i T_{0R}\times\\&\times\sum_{\substack{m=1\\ m\ odd}}^{M}\left(\prod_{p=1}^{m-1}R_{pR}\right)\exp\left(-jk_d\rho'\sin\theta_{mR}^i\right)\left(1+R_{mR}\right)\end{aligned} \tag{10}$$

where ρ' denotes the radial distance from the integration (source) point to the edge. Note that the electric and magnetic PO equivalent surface current densities can be expressed in compact form as:

$$\underline{J}_s(\rho')=\hat{J}_s\,E_0^i\sum_n A_n\exp\left(j\varphi_n(\rho')\right) \tag{11}$$

$$\underline{J}_{ms}(\rho')=\hat{J}_{ms}\,E_0^i\sum_n B_n\exp\left(j\varphi_n(\rho')\right) \tag{12}$$

If the approximation $\hat{R}\cong\hat{r}$ is adopted in the square brackets and accepted to have no effect on $G(R)$, the expression (6) can be re-arranged for each observation region:

$$\begin{aligned}\underline{E}^s\cong&-jkE_0^i\sum_{n\,even}\left[\left(\underline{\underline{I}}-\hat{r}\hat{r}\right)\left(\zeta\,A_{0_n}\right)\hat{J}_{s_0}+B_{0_n}\,\hat{J}_{ms_0}\times\hat{r}\right]\times\\&\times\iint_{S_0}\exp\left(j\varphi_{0_n}\right)G(R_0)\,dS_0+\\&-jkE_0^i\sum_{n\ odd}\left[\left(\underline{\underline{I}}-\hat{r}\hat{r}\right)\left(\zeta\,A_{\alpha_n}\right)\hat{J}_{s_\alpha}+B_{\alpha_n}\,\hat{J}_{ms_\alpha}\times\hat{r}\right]\times\\&\times\iint_{S_\alpha}\exp\left(j\varphi_{\alpha_n}\right)G(R_\alpha)\,dS_\alpha\end{aligned} \tag{13}$$

The above integrals can be manipulated according to [16]-[18] and reduced to a standard form suitable for the application of the Steepest Descent Method. Uniform asymptotic evaluations then lead to the expressions of the FD-UAPO diffraction coefficients *D* reported in the following.

A. $0 < \phi' < \pi/2$

A1. Internal region

$$\underline{E}^d_{\Omega_d} = D^{in}\frac{\exp(-jk_d\rho)}{\sqrt{\rho}}E_0^i\hat{z} = \frac{\exp(-jk_d\rho)}{\sqrt{\rho}}E_0^i\hat{z}\times$$
$$\times T_{0L}\left[D^{in}_{L_{S_0}} + D^{in}_{L_{S_\alpha}} + \Gamma(N)\left(D^{in}_{R_{S_0}} + D^{in}_{R_{S_\alpha}}\right)\right] \quad (14)$$

wherein

$$D^{in}_{L_{S_0}} = \frac{\exp(-j\pi/4)}{2\sqrt{2\pi k_d}}\left\{\left(\sin\phi - \cos\theta^t_{0L}\right)\times\right.$$
$$\times F\left(k_d,\rho,2\pi-\phi,\pi/2-\theta^t_{0L}\right) +$$
$$+\sum_{\substack{n=1\\ n\ even}}^{N}\left[\left(1+R_{nL}\right)\sin\phi + \left(1-R_{nL}\right)\cos\theta^i_{nL}\right]\prod_{p=1}^{n-1}R_{pL}\times \quad (15)$$
$$\left.\times F\left(k_d,\rho,2\pi-\phi,\pi/2-\theta^i_{nL}\right)\right\}$$

$$D^{in}_{L_{S_\alpha}} = \frac{\exp(-j\pi/4)}{2\sqrt{2\pi k_d}}\times$$
$$\times\sum_{\substack{n=1\\ n\ odd}}^{N}\left[\left(1-R_{nL}\right)\cos\theta^i_{nL} - \left(1+R_{nL}\right)\sin\left(\phi+\alpha\right)\right]\times \quad (16)$$
$$\times F\left(k_d,\rho,\phi-(2\pi-\alpha),\pi/2-\theta^i_{nL}\right)\prod_{p=1}^{n-1}R_{pL}$$

$$D^{in}_{R_{S_0}} = \frac{\exp(-j\pi/4)}{2\sqrt{2\pi k_d}}\left\{\left(\sin\phi - \cos\theta^t_{0R}\right)\times\right.$$
$$\times F\left(k_d,\rho,2\pi-\phi,\pi/2+\theta^t_{0R}\right) +$$
$$+\sum_{\substack{m=1\\ m\ even}}^{M}\left[\left(1+R_{mR}\right)\sin\phi + \left(1-R_{mR}\right)\cos\theta^i_{mR}\right]\prod_{p=1}^{m-1}R_{pR}\times \quad (17)$$
$$\left.\times F\left(k_d,\rho,2\pi-\phi,\pi/2+\theta^i_{mR}\right)\right\}$$

$$D^{in}_{R_{S_\alpha}} = \frac{\exp(-j\pi/4)}{2\sqrt{2\pi k_d}}\times$$
$$\times\sum_{\substack{m=1\\ m\ odd}}^{M}\left[(1-R_{mR})\cos\theta^i_{mR} - (1+R_{mR})\sin(\phi+\alpha)\right]\times \quad (18)$$
$$\times F\left(k_d,\rho,\phi-(2\pi-\alpha),\pi/2+\theta^i_{mR}\right)\prod_{p=1}^{m-1}R_{pR}$$

with

$$F(k,\rho,u,v) = \frac{F_t\left(2k\rho\cos^2\left(\frac{u+v}{2}\right)\right)}{\cos u + \cos v} \quad (19)$$

which contains the UTD transition function $F_t(\cdot)$ [2].

A2. External region

$$\underline{E}^d_{\Omega} = D^{out}\frac{\exp(-jk_0\rho)}{\sqrt{\rho}}E_0^i\hat{z} = \frac{\exp(-jk_0\rho)}{\sqrt{\rho}}E_0^i\hat{z}\times$$
$$\times T_{0L}\left[D^{out}_{L_{S_0}} + D^{out}_{L_{S_\alpha}} + \Gamma(N)\left(D^{out}_{R_{S_0}} + D^{out}_{R_{S_\alpha}}\right) + \frac{DI+DR}{T_{0L}}\right] \quad (20)$$

wherein

$$D^{out}_{L_{S_0}} = -\frac{\exp(-j\pi/4)}{2\sqrt{2\pi k_0}}\times$$
$$\times\sum_{\substack{n=1\\ n\ even}}^{N+1}T_{nL}\left[\sin\phi + \cos\theta^t_{nL}\right]\prod_{p=1}^{n-1}R_{pL}\times \quad (21)$$
$$\times F\left(k_0,\rho,\phi,\pm\left(\pi/2-\theta^t_{nL}\right)\right)U\left(\theta_c-\theta^i_{nL}\right)$$

$$D^{out}_{L_{S_\alpha}} = \frac{\exp(-j\pi/4)}{2\sqrt{2\pi k_0}}\times$$
$$\times\sum_{\substack{n=1\\ n\ odd}}^{N+1}T_{nL}\left[\sin\left(\phi+\alpha\right) - \cos\theta^t_{nL}\right]\prod_{p=1}^{n-1}R_{pL}\times \quad (22)$$
$$\times F\left(k_0,\rho,\phi+\alpha,\pm\left(\pi/2-\theta^t_{nL}\right)\right)U\left(\theta_c-\theta^i_{nL}\right)$$

$$D^{out}_{R_{S_0}} = -\frac{\exp(-j\pi/4)}{2\sqrt{2\pi k_0}}\times$$
$$\times\sum_{\substack{m=1\\ m\ even}}^{M}T_{mR}\left[\sin\phi + \cos\theta^t_{mR}\right]\prod_{p=1}^{m-1}R_{pR}\times \quad (23)$$
$$\times F\left(k_0,\rho,\phi,\pm(\pi/2+\theta^t_{mR})\right)U\left(\theta_c-\theta^i_{mR}\right)$$

$$D^{out}_{R_{S_\alpha}} = \frac{\exp(-j\pi/4)}{2\sqrt{2\pi k_0}}\times$$
$$\times\sum_{\substack{m=1\\ m\ odd}}^{M}T_{mR}\left[\sin\left(\phi+\alpha\right) - \cos\theta^t_{mR}\right]\prod_{p=1}^{m-1}R_{pR}\times \quad (24)$$
$$\times F\left(k_0,\rho,\phi+\alpha,\pm(\pi/2+\theta^t_{mR})\right)U\left(\theta_c-\theta^i_{mR}\right)$$

$$DI + DR = \left[(1 - R_{0L})\sin\phi' - (1 + R_{0L})\sin\phi\right] \times \\ \times F\left(k_0, \rho, \phi, \pm\phi'\right) \tag{25}$$

The sign + (–) in (21), (23), and (25) applies if $0 < \phi < \pi$ ($\pi < \phi < 2\pi - \alpha$), whereas the sign + (–) in (22) and (24) must be considered if $\pi - \alpha < \phi < 2\pi - \alpha$ ($0 < \phi < \pi - \alpha$).

B. $\pi/2 < \phi' < \pi - \alpha$

B1. Internal region

$$\underline{E}^d_{\Omega_d} = T_{0R}\left[D^{in}_{R_{S_0}} + D^{in}_{R_{S_\alpha}}\right]\frac{\exp(-jk_d\rho)}{\sqrt{\rho}}\,E^i_0\,\hat{z} \tag{26}$$

B2. External region

$$\underline{E}^d_{\Omega} = T_{0R}\left[D^{out}_{R_{S_0}} + D^{out}_{R_{S_\alpha}} + \frac{DI + DR}{T_{0R}}\right]\frac{\exp(-jk_0\rho)}{\sqrt{\rho}}\,E^i_0\,\hat{z} \tag{27}$$

Note that the expressions (26) and (27), which were proposed in [18], are a part of (14) and (20). These last provide the complete solutions for calculating the FD-UAPO coefficients related to the plane wave diffraction from an arbitrary-angled lossless wedge.

C. $\pi - \alpha < \phi' < \pi$

The waves penetrate into the wedge through S_0 and S_α, and travel outwards from the apex undergoing reflections and transmissions. Accordingly, the same formulation used for the case *B* can be adopted for the waves penetrating each surface.

The effectiveness of the FD-UAPO solutions has been tested by means of numerical simulations. The here reported results are relevant to the case *A* since numerical tests concerning the case *B* have been proposed in [18].

The first example refers to the wedge characterized by $\alpha = 30°$ and $\varepsilon_r = 3$. The incidence direction is fixed by $\phi' = 30°$ so that $\theta^t_{0L} = 30°$ and $N = M = 1$. The choice of this particular case is due to the simple characterization of the GO field contributions. In fact, the transmitted rays propagate into the wedge and normally impact on S_α ($\theta^i_{1L} = \theta^t_{1L} = 0°$). As a consequence, an external shadow boundary associated to the transmitted-transmitted rays appears at $\phi = 240°$. The rays reflected from S_α come back and impinge on the internal face of S_0 with $\theta^i_{2L} = 30°$. Accordingly $\theta^t_{2L} = 60°$ and a further external shadow boundary due to the transmitted-reflected-transmitted rays exists at $\phi = 30°$. The related internal reflection angle is $\theta^r_{2L} = \theta^t_{0R} = 30°$ and then $\theta^i_{1R} = 60° > \theta_c$, namely, no more external shadow boundaries occur. Note that the corresponding reflected rays propagate parallel to S_0. Accordingly, the GO field possesses four external shadow boundaries (i.e., $\phi = 30°, 150°, 210°, 240°$) and one GO field boundary exists at $\phi = 0°/360°$. The FD-UAPO diffracted field is significant near to such directions (see Fig. 4a) and its jumps are opposite to the GO jumps at the boundaries (see Fig. 4b). It is able to compensate all the GO field discontinuities in the internal and external observation domains, thus obtaining a continuous total field as shown in Fig. 5. The data are collected on the circular path with radius $\rho = 4\lambda_0$, λ_0 being the free-space wavelength.

Figures 6 and 7 show the comparisons with numerical data obtained by using a FDTD code, which implements the total field/scattered field technique [26]. A normalized dB scale is adopted to compare the results. The first figure refers to the previous test case, whereas the latter is relevant to a wedge characterized by $\alpha = 20°$ and $\varepsilon_r = 2$ when the plane wave impinges at $\phi' = 60°$. A good agreement is evident both in Ω and Ω_d, thus assessing the effectiveness of the FD-UAPO solutions. Some FDTD data lie outside the UAPO curve as expected since the proposed solutions suffer from the PO approximation and neglect the surface waves.

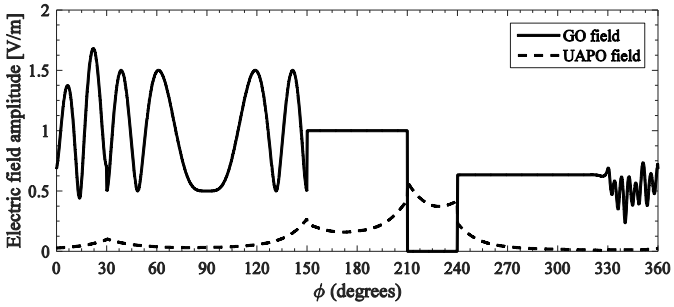

Fig. 4a. Amplitude of the GO and FD-UAPO field contributions. Wedge parameters: $\alpha = 30°$, $\varepsilon_r = 3$. Incident field: $E^i_0 = 1$. Incidence direction: $\phi' = 30°$. Observation path: $\rho = 4\lambda_0$.

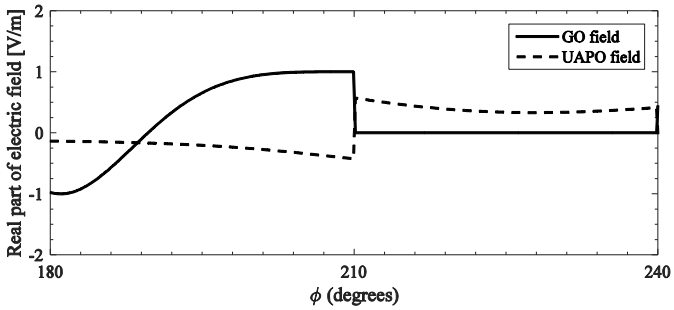

Fig. 4b. Real part of the GO and FD-UAPO field contributions at the shadow boundary of the incident field. Wedge parameters: $\alpha = 30°$, $\varepsilon_r = 3$. Incident field: $E^i_0 = 1$. Incidence direction: $\phi' = 30°$. Observation path: $\rho = 4\lambda_0$.

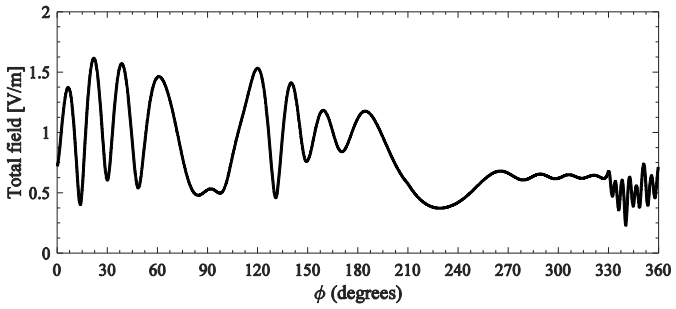

Fig. 5. Amplitude of the total field. Wedge parameters: $\alpha = 30°$, $\varepsilon_r = 3$. Incident field: $E_0^i = 1$. Incidence direction: $\phi' = 30°$. Observation path: $\rho = 4\lambda_0$.

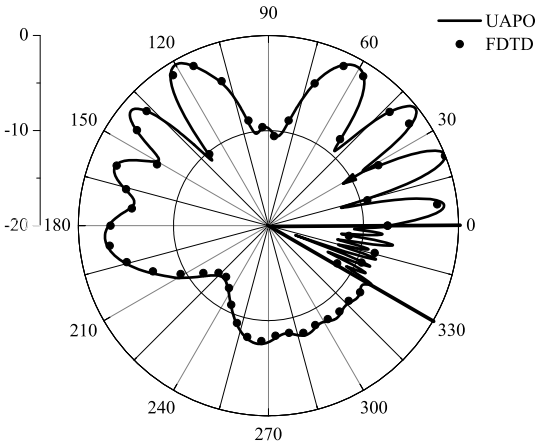

Fig. 6. Comparison with FDTD data. Wedge parameters: $\alpha = 30°$, $\varepsilon_r = 3$. Incident field: $E_0^i = 1$. Incidence direction: $\phi' = 30°$. Observation path: $\rho = 4\lambda_0$.

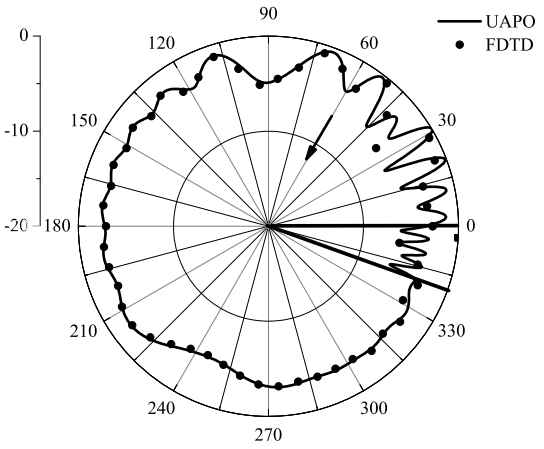

Fig. 7. Comparison with FDTD data. Wedge parameters: $\alpha = 20°$, $\varepsilon_r = 2$. Incident field: $E_0^i = 1$. Incidence direction: $\phi' = 60°$. Observation path: $\rho = 4\lambda_0$.

IV. TD-UAPO Diffracted Field

The TD-UAPO diffraction coefficients *d* are determined by applying the inverse Laplace transform to the FD-UAPO counterparts under the hypothesis that the dielectric parameters are independent on the frequency. Their knowledge allows one to evaluate the transient diffracted field e^d due to an arbitrary function plane wave with the incident field e^i (forcing function) turned on at $t = t_0$, i.e.,

$$e^d(P,t) = \frac{1}{\sqrt{\rho}} \int_{t_0}^{t-\rho/c} d\left(t - \frac{\rho}{c} - \tau\right) e^i(O,\tau)\,\mathrm{d}\tau \qquad t - \frac{\rho}{c} > t_0 \quad (28)$$

where *c* is the speed of light.

The TD-UAPO expressions to evaluate *d* are reported in the following by applying the same scheme adopted in the previous section.

A. $0 < \phi' < \pi/2$

A1. Internal region

$$\begin{aligned} d^{in} &= L^{-1}\left(D^{in}\right) = \\ &= T_{0L}\left[d^{in}_{L_{S_0}} + d^{in}_{L_{S_\alpha}} + \Gamma(N)\left(d^{in}_{R_{S_0}} + d^{in}_{R_{S_\alpha}}\right)\right] \end{aligned} \quad (29)$$

wherein

$$\begin{aligned} d^{in}_{L_{S_0}} &= \frac{1}{2\sqrt{2\pi}} \left\{\left(\sin\phi - \cos\theta^t_{0L}\right)\times\right. \\ &\times G\left(X\left(\rho, 2\pi - \phi, \pi/2 - \theta^t_{0L}\right), t\right) + \\ &+ \sum_{\substack{n=1 \\ n\ even}}^{N} \left[\left(1 + R_{nL}\right)\sin\phi + \left(1 - R_{nL}\right)\cos\theta^i_{nL}\right] \prod_{p=1}^{n-1} R_{pL} \times \\ &\left.\times G\left(X\left(\rho, 2\pi - \phi, \pi/2 - \theta^i_{nL}\right), t\right)\right\} \end{aligned} \quad (30)$$

$$\begin{aligned} d^{in}_{L_{S_\alpha}} &= \frac{1}{2\sqrt{2\pi}} \sum_{\substack{n=1 \\ n\ odd}}^{N} \prod_{p=1}^{n-1} R_{pL} \times \\ &\times\left[\left(1 - R_{nL}\right)\cos\theta^i_{nL} - \left(1 + R_{nL}\right)\sin\left(\phi + \alpha\right)\right]\times \\ &\times G\left(X\left(\rho, \phi - (2\pi - \alpha), \pi/2 - \theta^i_{nL}\right), t\right) \end{aligned} \quad (31)$$

$$d^{in}_{R_{S_0}} = \frac{1}{2\sqrt{2\pi}} \left\{ \left(\sin\phi - \cos\theta^t_{0R} \right) \times \right.$$
$$\times G\left(X\left(\rho, 2\pi - \phi, \pi/2 + \theta^t_{0R} \right), t \right) +$$
$$+ \sum_{\substack{m=1 \\ m\ even}}^{M} \left[\left(1 + R_{mR}\right) \sin\phi + \left(1 - R_{mR}\right) \cos\theta^i_{mR} \right] \prod_{p=1}^{m-1} R_{pR} \times \quad (32)$$
$$\left. \times G\left(X\left(\rho, 2\pi - \phi, \pi/2 + \theta^i_{mR} \right), t \right) \right\}$$

$$d^{in}_{R_{S_\alpha}} = \frac{1}{2\sqrt{2\pi}} \sum_{\substack{m=1 \\ m\ odd}}^{M} \prod_{p=1}^{m-1} R_{pR} \times$$
$$\times \left[(1 - R_{mR}) \cos\theta^i_{mR} - (1 + R_{mR}) \sin(\phi + \alpha) \right] \times \quad (33)$$
$$\times G\left(X\left(\rho, \phi - (2\pi - \alpha), \pi/2 + \theta^i_{mR} \right), t \right)$$

with

$$G\left(X\left(\rho, u, v \right), t \right) = \frac{1}{\cos u + \cos v} \frac{X\left(\rho, u, v \right)}{\sqrt{\pi c t} \left[t + X\left(\rho, u, v \right)/c \right]} \quad (34)$$

$$X\left(\rho, u, v \right) = 2\rho \cos^2\left(\frac{u+v}{2} \right) \quad (35)$$

A2. External region

$$d^{out} = L^{-1}\left(D^{out} \right) =$$
$$= T_{0L} \left[d^{out}_{L_{S_0}} + d^{out}_{L_{S_\alpha}} + \Gamma\left(N \right) \left(d^{out}_{R_{S_0}} + d^{out}_{R_{S_\alpha}} \right) + \frac{di + dr}{T_{0L}} \right] \quad (36)$$

wherein

$$d^{out}_{L_{S_0}} = -\frac{1}{2\sqrt{2\pi}} \sum_{\substack{n=1 \\ n\ even}}^{N+1} T_{nL} \left[\sin\phi + \cos\theta^t_{nL} \right] \prod_{p=1}^{n-1} R_{pL} \times$$
$$\times G\left(X\left(\rho, \phi, \pm\left(\pi/2 - \theta^t_{nL} \right) \right), t \right) U\left(\theta_c - \theta^i_{nL} \right) \quad (37)$$

$$d^{out}_{L_{S_\alpha}} = \frac{1}{2\sqrt{2\pi}} \sum_{\substack{n=1 \\ n\ odd}}^{N+1} T_{nL} \left[\sin\left(\phi + \alpha \right) - \cos\theta^t_{nL} \right] \times$$
$$\times G\left(X\left(\rho, \phi + \alpha, \pm\left(\pi/2 - \theta^t_{nL} \right) \right), t \right) U\left(\theta_c - \theta^i_{nL} \right) \prod_{p=1}^{n-1} R_{pL} \quad (38)$$

$$d^{out}_{R_{S_0}} = -\frac{1}{2\sqrt{2\pi}} \sum_{\substack{m=1 \\ m\ even}}^{M} T_{mR} \left[\sin\phi + \cos\theta^t_{mR} \right] \prod_{p=1}^{m-1} R_{pR} \times$$
$$\times G\left(X\left(\rho, \phi, \pm(\pi/2 + \theta^t_{mR}) \right), t \right) U\left(\theta_c - \theta^i_{mR} \right) \quad (39)$$

$$d^{out}_{R_{S_\alpha}} = \frac{1}{2\sqrt{2\pi}} \sum_{\substack{m=1 \\ m\ odd}}^{M} T_{mR} \left[\sin\left(\phi + \alpha \right) - \cos\theta^t_{mR} \right] \times$$
$$\times G\left(X\left(\rho, \phi + \alpha, \pm(\pi/2 + \theta^t_{mR}) \right), t \right) U\left(\theta_c - \theta^i_{mR} \right) \prod_{p=1}^{m-1} R_{pR} \quad (40)$$

$$di + dr = \left[(1 - R_{0L}) \sin\phi' - (1 + R_{0L}) \sin\phi \right] \times$$
$$\times G\left(X\left(\rho, \phi, \pm\phi' \right), t \right) \quad (41)$$

B. $\pi/2 < \phi' < \pi - \alpha$

B1. Internal region

$$d^{in} = T_{0R} \left[d^{in}_{R_{S_0}} + d^{in}_{R_{S_\alpha}} \right] \quad (42)$$

B2. External region

$$d^{out} = T_{0R} \left[d^{out}_{R_{S_0}} + d^{out}_{R_{S_\alpha}} + \frac{di + dr}{T_{0R}} \right] \quad (43)$$

C. $\pi - \alpha < \phi' < \pi$

The solutions proposed for the case *B* can be again used for the waves penetrating S_0, whereas analogous expressions can be derived for the waves going through S_α.

V. Conclusions

The diffraction problem relevant to an arbitrary-angled lossless dielectric wedge with planar surfaces has been tackled and solved in frequency and time domains. The corresponding UAPO diffraction coefficients are formulated in terms of the GO response of the structure and are efficient from the computational viewpoint since expressed in explicit closed form. The UAPO diffracted field compensates the GO discontinuities and gives a quite accurate total field, even if it possess some limitations due to the PO approximation applied to involved surface currents.

It must be stressed that the presented analysis provides one of the most elaborated solutions for evaluating the UAPO diffraction coefficients related to the plane wave diffraction by an arbitrary-angled lossless wedge.

REFERENCES

[1] J.B. Keller, "Geometrical theory of diffraction," *J. Opt. Am.*, vol. 52, pp. 116-130, 1962.

[2] R. G. Kouyoumjian and P. H. Pathak, "A uniform geometrical theory of diffraction for an edge in a perfectly conducting surface," *Proc. IEEE*, vol. 62, pp. 1448-1461, 1974.

[3] S. Berntsen, "Diffraction of an electric polarized wave by a dielectric wedge," *SIAM J. Appl. Math.*, vol. 43, pp. 186-211, 1983.

[4] A. D. Rawlins, "Diffraction by, or diffusion into, a penetrable wedge," *Proc. R. Soc. Lond. A*, vol. 455, pp. 2655-2686, 1999.

[5] R. E. Burge *et al.*, "Microwave scattering from dielectric wedges with planar surfaces: a diffraction coefficient based on a physical optics version of GTD," *IEEE Trans. Antennas Propagat.*, vol. 47, pp. 1515-1527, 1999.

[6] J. F. Rouviere, N. Douchin, and P. F. Combes, "Diffraction by lossy dielectric wedges using both heuristic UTD formulations and FDTD," *IEEE Trans. Antennas Propagat.*, vol. 47, pp. 1702-1708, 1999.

[7] C. H. Seo and J. W. Ra, "Plane wave scattering by a lossy dielectric wedge," *Microwave Opt. Technol. Lett.*, vol. 25, 360-363, 2000.

[8] S. Y. Kim, J. W. Ra, and S. Y. Shin, "Diffraction by an arbitrary-angled dielectric wedge: part I–physical optics approximation," *IEEE Trans. Antennas Propagat.*, vol. 39, pp. 1272-1281, 1991.

[9] S. Y. Kim, J. W. Ra, and S. Y. Shin, "Diffraction by an arbitrary-angled dielectric wedge: part II–physical optics approximation," *IEEE Trans. Antennas Propagat.*, vol. 39, pp. 1272-1281, 1991.

[10] P. Bernardi, R. Cicchetti, and O. Testa, "A three-dimensional UTD heuristic diffraction coefficient for complex penetrable wedges," *IEEE Trans. Antennas Propagat.*, vol. 50, pp. 217-224, 2002.

[11] M. A. Salem, A. H. Kamel, and A. V. Osipov, "Electromagnetic fields in presence of an infinite dielectric wedge," *Proc. R. Soc. Lond.* A, vol. 462, pp. 2503-2522, 2006.

[12] V. Daniele and G. Lombardi, "The Wiener-Hopf solution of the isotropic penetrable wedge problem: diffraction and total field," *IEEE Trans. Antennas Propagat.*, vol. 59, pp. 3797-3818, 2011.

[13] E. N. Vasilev and V. V. Solodukhov, "Diffraction of electromagnetic waves by a dielectric wedge, " *Radiophysics and Quantum Electronics,* vol. 17, pp. 1161-1169, 1976.

[14] E. N. Vasilev, V. V. Solodukhov, and A. I. Fedorenko, "The Integral Equation Method in the Problem of Electromagnetic Waves Diffraction by Complex Bodies," *Electromagnetics*, vol. 11, 161-182, 1991.

[15] B. Budaev, *Diffraction by Wedges*. London: Longman Scient, 1995.

[16] G. Gennarelli and G. Riccio, "A uniform asymptotic solution for diffraction by a right-angled dielectric wedge," *IEEE Trans. Antennas Propagat.*, vol. 59, pp. 898-903, 2011.

[17] G. Gennarelli and G. Riccio, "Plane-wave diffraction by an obtuse-angled dielectric wedge," *J. Opt. Soc. Am. A*, vol. 28, pp. 627-632, 2011.

[18] G. Gennarelli, M. Frongillo, and G. Riccio, "High-frequency evaluation of the field inside and outside an acute-angled dielectric wedge," *IEEE Trans. Antennas Propagat.*, vol. 63, pp. 374-378, 2015.

[19] G. Gennarelli and G. Riccio, "Time domain diffraction by a right-angled penetrable wedge," *IEEE Trans. Antennas Propagat.*, vol. 60, pp. 2829-2833, 2012.

[20] G. Gennarelli and G. Riccio, "Obtuse-angled penetrable wedges: a time domain solution for the diffraction coefficients," *J. Electromagn. Waves Appl.*, vol. 27, pp. 2020-2028, 2013.

[21] T. W. Veruttipong, "Time domain version of the uniform GTD," *IEEE Trans. Antennas Propagat.*, vol. 38, pp. 1757-1764, 1990.

[22] M. Frongillo, G. Gennarelli, and G. Riccio, "TD-UAPO diffracted field evaluation for penetrable wedges with acute apex angle," *J. Opt. Soc. Am. A*, vol. 32, pp. 1271-1275, 2015.

[23] G. Gennarelli and G. Riccio, "Diffraction by 90° penetrable wedges with finite conductivity," *J. Opt. Soc. Am. A*, vol. 31, pp. 21-25, 2014.

[24] M. Frongillo, G. Gennarelli, and G. Riccio, "Diffraction by arbitrary-angled dielectric wedges: closed form high-frequency solutions," in *Proc. 2015 Progress in Electromagnetics Research Symp.*, Prague (Czech Republic), pp. 964-967.

[25] M. Frongillo, G. Gennarelli, and G. Riccio, "TD-UAPO diffraction coefficients for wedges with arbitrary apex angle," in *Proc. 2015 Int. Symp. on Microwave and Optical Tech.*, Dresda (Germany), pp. 1-4.

[26] A. Taflove and S. Hagness, *Computational Electrodynamics: The Finite Difference Time Domain Method*. Norwood: Artech House, 2000.

Giovanni Riccio received the Laurea degree in Electronic Engineering from the University of Salerno, Italy. From 1995 to 2001 he was Assistant Professor at the Engineering Faculty of the University of Salerno, where he is currently Associate Professor of Electromagnetics. His research activity concerns nonredundant sampling representations of electromagnetic fields, near field – far field transformation techniques, radar cross section of corner reflectors, wave scattering from penetrable and impenetrable structures. Giovanni Riccio is co-author of about 250 scientific papers, mainly in international journals and conference proceedings. He is a Member of the IEEE Society and Fellow of the Electromagnetics Academy.

Gianluca Gennarelli was born in Avellino, Italy, in 1981. He received the M.Sc. degree (*summa cum laude*) in electronic engineering and the Ph.D. degree in information engineering at the University of Salerno, Salerno, Italy, in 2006 and 2010, respectively.
He held a Post-Doctoral Fellowship at the University of Salerno from April 2010 to December 2011. Since January 2012, he has been a research scientist at the Institute for Electromagnetic Sensing of the Environment of the Italian National Research Council (IREA-CNR), Napoli, Italy. In 2015, he has been a visiting scientist at the North Atlantic Treaty Organization (NATO) Science & Technology Organization (STO) Centre for Maritime Research and Experimentation (CMRE), La Spezia, Italy.
His research interests cover theoretical and applied electromagnetic topics such as microwave sensors, antennas, electromagnetic inverse scattering problems, radar imaging, diffraction problems, near-field far-field transformation techniques, and electromagnetic simulation.
Dr. Gennarelli has co-authored over hundred publications in international peer-reviewed journals and conference proceedings. He serves as a technical reviewer for international journals and conferences in the field of antennas and propagation, remote sensing, optics, signal processing, and applied physics.

Marcello Frongillo was born in Avellino, Italy, in 1982. He received the Master's degree in Engineering of the Telecommunications from the University Federico II, Naples, in 2010. Since 2012 he has been Ph.D. student on Applied Electromagnetics and received the Ph.D. degree in Information Engineering from the University of Salerno, in 2016. His research work involves high-frequency asymptotic techniques and numerical approaches to diffraction problems.